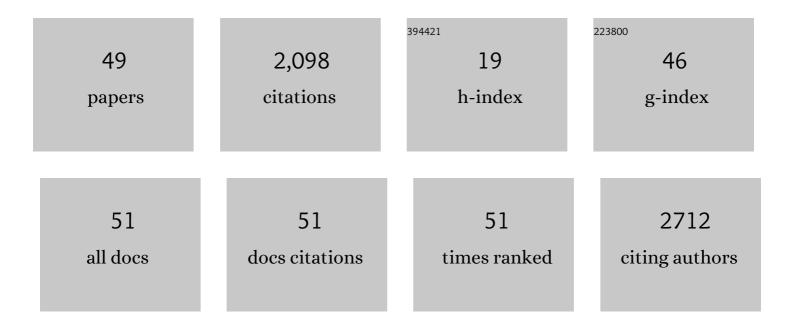
Yong Chan Choi

List of Publications by Year in descending order

Source: https://exaly.com/author-pdf/8027823/publications.pdf Version: 2024-02-01



#	Article	IF	CITATIONS
1	Compositional Engineering of Antimony Chalcoiodides via a Two-Step Solution Process for Solar Cell Applications. ACS Applied Energy Materials, 2022, 5, 5348-5355.	5.1	13
2	Photovoltaic Performance of Dye-Sensitized Solar Cells with a Solid-State Redox Mediator Based on an Ionic Liquid and Hole-Transporting Triphenylamine Compound. Energies, 2022, 15, 2765.	3.1	3
3	One-Step Solution Deposition of Antimony Selenoiodide Films via Precursor Engineering for Lead-Free Solar Cell Applications. Nanomaterials, 2021, 11, 3206.	4.1	11
4	Recent Progress in Fabrication of Antimony/Bismuth Chalcohalides for Lead-Free Solar Cell Applications. Nanomaterials, 2020, 10, 2284.	4.1	22
5	Molecular Weight Effects of Biscarbazole-Based Hole Transport Polymers on the Performance of Solid-State Dye-Sensitized Solar Cells. Nanomaterials, 2020, 10, 2516.	4.1	5
6	Enhanced Power Conversion Efficiency of Dye-Sensitized Solar Cells by Band Edge Shift of TiO2 Photoanode. Molecules, 2020, 25, 1502.	3.8	11
7	Efficient Nanostructured TiO ₂ /SnS Heterojunction Solar Cells. Advanced Energy Materials, 2019, 9, 1901343.	19.5	86
8	Enhanced performance of perovskite solar cells by incorporation of a triphenylamine derivative into hole-transporting poly(3-hexylthiophene) layers. Journal of Industrial and Engineering Chemistry, 2019, 73, 175-181.	5.8	19
9	Controlled Growth of BiSI Nanorod-Based Films through a Two-Step Solution Process for Solar Cell Applications. Nanomaterials, 2019, 9, 1650.	4.1	21
10	Morphology Transformation of Chalcogenide Nanoparticles Triggered by Cation Exchange Reactions. Chemistry of Materials, 2019, 31, 268-276.	6.7	12
11	Efficient Solar Cells Based on Lightâ€Harvesting Antimony Sulfoiodide. Advanced Energy Materials, 2018, 8, 1701901.	19.5	76
12	Controlled growth of SbSI thin films from amorphous Sb2S3 for low-temperature solution processed chalcohalide solar cells. APL Materials, 2018, 6, .	5.1	29
13	Key Factors Affecting the Performance of Sb ₂ S ₃ -sensitized Solar Cells During an Sb ₂ S ₃ Deposition via SbCl ₃ -thiourea Complex Solution-processing. Journal of Visualized Experiments,	0.3	2
14	Antisolvent-assisted powder engineering for controlled growth of hybrid CH3NH3PbI3 perovskite thin films. APL Materials, 2017, 5, .	5.1	25
15	Effects of a TiO 2 :CaO barrier layer on the back electron transfer in TiO 2 -based solar cells. Journal of Industrial and Engineering Chemistry, 2017, 50, 96-101.	5.8	10
16	Systematic control of nanostructured interfaces of planar Sb 2 S 3 solar cells by simple spin-coating process and its effect on photovoltaic properties. Journal of Industrial and Engineering Chemistry, 2017, 56, 196-202.	5.8	24
17	Controlled growth of organic–inorganic hybrid CH ₃ NH ₃ PbI ₃ perovskite thin films from phase-controlled crystalline powders. RSC Advances, 2016, 6, 104359-104365.	3.6	16
18	Effects of pyrolysis temperature on structural, Raman, and infrared properties of perovskite PbTiO3 nanotubes. Journal of the Korean Physical Society, 2016, 68, 545-550.	0.7	2

#	Article	IF	CITATIONS
19	Efficient Sb ₂ S ₃ â€Sensitized Solar Cells Via Singleâ€Step Deposition of Sb ₂ S ₃ Using S/Sbâ€Ratioâ€Controlled SbCl ₃ â€Thiourea Complex Solution. Advanced Functional Materials, 2015, 25, 2892-2898.	14.9	145
20	CuSbS ₂ ‣ensitized Inorganic–Organic Heterojunction Solar Cells Fabricated Using a Metal–Thiourea Complex Solution. Angewandte Chemie - International Edition, 2015, 54, 4005-4009.	13.8	72
21	Efficient room temperature aqueous Sb ₂ S ₃ synthesis for inorganic–organic sensitized solar cells with 5.1% efficiencies. Chemical Communications, 2015, 51, 8640-8643.	4.1	78
22	Sb ₂ Se ₃ â€Sensitized Inorganic–Organic Heterojunction Solar Cells Fabricated Using a Singleâ€Source Precursor. Angewandte Chemie - International Edition, 2014, 53, 1329-1333.	13.8	145
23	Efficient Inorganicâ€Organic Heterojunction Solar Cells Employing Sb ₂ (S _{<i>x</i>/sub>/Se_{1â€<i>x</i>})₃ Gradedâ€Composition Sensitizers. Advanced Energy Materials, 2014, 4, 1301680.}	19.5	123
24	Highly Improved Sb ₂ S ₃ Sensitizedâ€Inorganic–Organic Heterojunction Solar Cells and Quantification of Traps by Deepâ€Level Transient Spectroscopy. Advanced Functional Materials, 2014, 24, 3587-3592.	14.9	454
25	Effects of Sintering Temperature on the Pyrochlore Phase in PZT Nanotubes and Their Transformation to the Perovskite Phase by Coating with PbO Multilayers. Journal of Nanoscience and Nanotechnology, 2014, 14, 8554-8560.	0.9	2
26	Nanostructured TiO2/CH3NH3PbI3 heterojunction solar cells employing spiro-OMeTAD/Co-complex as hole-transporting material. Journal of Materials Chemistry A, 2013, 1, 11842.	10.3	301
27	Photoluminescence of ultra-thin-walled Pb(Zr,Ti)O3 nanotubes synthesized in the porous alumina membrane template-directed method. Journal of the Korean Physical Society, 2013, 63, 1040-1044.	0.7	3
28	Strong pore-size dependence of the optical properties in porous alumina membranes. Journal of the Korean Physical Society, 2013, 63, 1789-1793.	0.7	6
29	Effects of Wall Thickness on Morphology and Structure of Lead Titanate Nanotubes. Ferroelectrics, 2013, 454, 29-34.	0.6	5
30	Effects of Anodization Time and Temperature on the Pore Arrangement of Porous Anodic Alumina Anodized in Sulfuric Acid. New Physics: Sae Mulli, 2013, 63, 1249-1253.	0.1	1
31	THE DEPENDENCE OF ALUMINA NANOWIRE FORMATION FROM POROUS ANODIC ALUMINA MEMBRANES ON THE ETCHING SOLUTION. Modern Physics Letters B, 2012, 26, 1150017.	1.9	1
32	Lubricating layer formed on porous anodic alumina template due to pore effect at water lubricated sliding and its properties. Thin Solid Films, 2012, 521, 3-6.	1.8	6
33	Paramagnetism in Pb(Zr,Ti)O3 nanotube arrays at low temperatures. Journal of the Korean Physical Society, 2012, 60, 1097-1101.	0.7	3
34	Effects of etching time on the bottom surface morphology of ultrathin porous alumina membranes for use as masks. Journal of the Korean Physical Society, 2012, 61, 1660-1665.	0.7	3
35	Surface-adsorbate-induced fluorescence-type Raman background of Pb(Zr0.4Ti0.6)O3 nanotubes. Current Applied Physics, 2012, 12, 1272-1277.	2.4	2
36	Tribological effects of pores on an anodized Al alloy surface as lubricant reservoir. Current Applied Physics, 2011, 11, S182-S186.	2.4	28

Yong Chan Choi

#	Article	IF	CITATIONS
37	Effects of a perfluorinated compound as an additive on the power conversion efficiencies of polymer solar cells. Solar Energy Materials and Solar Cells, 2011, 95, 1908-1914.	6.2	26
38	Nanopore Domain Growth Behavior by Nanopore Changes Near Domain Boundaries in Porous Anodic Alumina. Journal of Nanoscience and Nanotechnology, 2011, 11, 1346-1349.	0.9	6
39	Effects of Thermal Treatment Conditions on the Phase Formation and the Morphological Changes of Sol-gel Derived 0.67Pb(Mg1/3Nb2/3)O3-0.33PbTiO3 Thin Films. Journal of the Korean Physical Society, 2011, 58, 668-673.	0.7	5
40	Synthesis of Metal-oxide Nanotubes by Using Template-directed Growth in Conjunction with the Sol-gel Process and a Spin-coating Technique. Journal of the Korean Physical Society, 2011, 59, 2551-2555.	0.7	7
41	?Correlation between Self-Organized Pore Formation Behaviors and Current-Time Characteristics in Porous Anodic Alumina: Quantitative Analysis of Voltage Dependence of Pore Morphological Changes. Journal of the Korean Physical Society, 2010, 56, 113-119.	0.7	10
42	Self-assembled growth of nanocomposites consisting of TiO2nanopillars and Pb(Zr0.52Ti0.48)O3thin films. Nanotechnology, 2009, 20, 425601.	2.6	1
43	Ferroelectricity in Highly Ordered Arrays of Ultra-Thin-Walled Pb(Zr,Ti)O ₃ Nanotubes Composed of Nanometer-Sized Perovskite Crystallites. Nano Letters, 2008, 8, 1813-1818.	9.1	112
44	Lead Zirconate Titanate Nanowire Growth Via Spin Coating in Conjunction with Sol-Gel Process. Ferroelectrics, 2007, 356, 230-235.	0.6	1
45	Synthesis and Characterization of Lead Zirconate Titanate Nanotubes. Ferroelectrics, 2007, 356, 236-241.	0.6	3
46	Structure of alumina nanowires synthesized by chemical etching of anodic alumina membrane. Physica E: Low-Dimensional Systems and Nanostructures, 2007, 36, 140-146.	2.7	19
47	Synthesis of Crystalline Lead Di-Oxide Nanowires and Their Electron-Beam-Induced Phase Transformation to Oxygen Deficient Lead Mono-Oxide. Journal of the Korean Physical Society, 2007, 51, 2045.	0.7	3
48	Template-directed formation of functional complex metal-oxide nanostructures by combination of sol–gel processing and spin coating. Materials Science and Engineering B: Solid-State Materials for Advanced Technology, 2006, 133, 245-249.	3.5	17
49	Direct observation of alumina nanowire formation from porous anodic alumina membrane via the droplet etching method. Nanotechnology, 2006, 17, 355-359.	2.6	52